Preprints of the 21st IFAC World Congress (Virtual)
Berlin, Germany, July 12-17, 2020

Multi-objective non linear dynamic model identification considering nearly optimal solutions. Application to a μ-CHP system based on PEMFC. ⋆

A. Pajares * **J.M. Herrero** * **X. Blasco** * **S. García-Nieto** *
J.V. Salcedo *

* *Instituto Universitario de Automática e Informática Industrial, Universitat Politècnica de València, Camino de Vera s/n, Valencia 46022, Spain (e-mail: juaherdu@isa.upv.es).*

Abstract: Solving a wide range of engineering problems can be approached from the point of view of multi-objective optimization (MOO), i.e. trying to optimize several conflicting objectives simultaneously. Solutions to these problems are not unique and the designer must choose from several optimal solutions (Pareto set), depending on his or her preferences. However, in addition to those solutions, there are almost optimal solutions that can be preferred for several reasons. For example, if the problem is multimodal, the optimization algorithm only offers one of the possible solutions. Furthermore, the problem may present a certain degree of simplification which implies that not all preferences are reflected in the minimization objectives. The nevMOGA algorithm (multiobjective genetic algorithm of the epsilon neighborhood variable) offers the possibility of finding, apart from an approximation to the Pareto optimal set, an extra set of potentially useful near optimal solutions. This result allows a final solution more closely aligned with the designer's actual preferences. This paper shows the application of this technique to the experimental identification problem of the parameters of a complex dynamic model. In particular, it is applied to identify the thermal model of a μ-CHP (micro Combined Heat and Power) system with a PEMFC (Proton Exchange Membrane Fuel Cell) type hydrogen cell.

Keywords: Multi-objective optimization, Non linear identification, multivariable identification, μ-CHP.

1. INTRODUCTION

A wide range of engineering problems can be solved from multi-objective optimization point of view, where it is necessary to optimize several conflicting objectives simultaneously. For instance, a typical problem is the model identification of multivariable dynamical systems. In these problems, the objectives to be optimized are related to the errors (in the different outputs) of the predictions of the model against the real data obtained experimentally. A multi-objective problem appears naturally as there are several outputs to adjust. Due the unmodeled dynamics, in general, there is no single optimum solution for adjusting all outputs simultaneously.

In a classic approach different objectives are usually aggregated, which means a decision (a priori) (Miettinen (1998)) and supplies a unique solution. All the detail about the performance balance between the different solutions is lost. A more general approach is to consider that the solution to these problems is not unique and the designer must choose (a posteriori) between several optimal solutions (Pareto set), the one that best matches his/her preferences (Coello et al. (2007)).

A novel approach is one that considers, in addition to optimal solutions, potentially useful nearly optimal solutions (Pajares et al. (2018)) known as nearly optimal not dominated in their neighborhood. These nearly optimal solutions have similar performance to the optimal ones but with difference in the parameter space.

These nearly optimal solutions allow:

- To extend the set of solutions of interest, with different solutions with good performance with respect to the optimized objectives.
- To detect multimodality.
- To obtain solutions better than the optimal ones when analyzing objectives not considered in the optimization process.

Considering the nearly optimal solutions allows the designer to make the final decision in a more informed way. These alternatives allow studying new indicators not included in the design objectives for optimal and nearly optimal solutions. Thus, the designer can reduce the design objectives, facilitating the convergence of the algorithm used, analyzing these indicators in the decision phase.

⋆ This work was supported in part by the Ministerio de Economía y Competitividad, Spain, under Grant RTI2018-096904-B-I00, and in part by the Local Administration Generalitat Valenciana under Project AICO/2019/055.

In order to show the benefits of this approach, the identification of the cooling system for a μ-CHP system (micro Combined Heat and Power) based on PEMFC (Proton Exchange Membrane Fuel Cell) presented in (Navarro Giménez et al. (2019)) is considered.

A μ-CHP system (Maghanki et al. (2013)) generates electricity and heat for the energy supply of a house. On the one hand, the electrical energy produced feeds the electrical loads of the house. On the other hand, the thermal energy generated is used for heating and hot water. The main advantage of these systems is the use of the thermal energy generated during the process of electricity production. A novel alternative in the design of this type of systems is to use a fuel cell as an electric generator and take advantage of the heat produced (Hawkes et al. (2009)). The correct design of the cooling system is key issue in the durability, cost, reliability and energy efficiency of the fuel cell (Schmittinger and Vahidi (2008)) and of course the μ-CHP system. However, in order to design a good temperature control of the PEMFC, it is necessary to have an adequate model of the cooling system.

Therefore, a complete dynamic model of the fuel cell cooling unit in a μ-CHP system is identified applying a MOO approach. As a novelty in the modeling procedure, nearly optimal solutions not dominated in its neighborhood are considered. The nevMOGA algorithm (Pajares et al. (2018)) will be used to characterize Pareto front and nearly optimal solutions. Thus, it will be shown how nearly optimal models can be better than optimal ones when model validation is considered or when new quality indicators are considered.

The remainder of this work is as follows: In Section 2 a brief background on MOO problem and the definition of the nearly optimal solutions non dominated in their neighborhood. In Section 3, the nevMOGA algorithm is briefly presented. In section 4, the model parameter identification of the cooling system of a μ-CHP process is shown. Finally, in Section 5 the main conclusions are presented.

2. MULTI-OBJECTIVE BACKGROUND

A general MOO problem can be stated as follows:

$$\min_{\boldsymbol{x}\in Q} \boldsymbol{f}(\boldsymbol{x}) \;\; s.t. \;\; constraints \tag{1}$$

where $\boldsymbol{x} = [x_1, ..., x_k]$ is defined as a decision vector in the domain $Q \subset \Re^k$ and $\boldsymbol{f}$: $Q \rightarrow \Re^m$ is defined as the vector of objective functions $\boldsymbol{f}(\boldsymbol{x}) = [f_1(\boldsymbol{x}), ..., f_m(\boldsymbol{x})]$. The domain Q is defined by the set of constraints on $\boldsymbol{x}$. For instance (but not limited to):

$$\underline{x_i} \leq x_i \leq \overline{x_i}, \; i = [1, ..., k] \tag{2}$$

$\underline{x_i}$ and $\overline{x_i}$ are the lower and upper bounds of $\boldsymbol{x}$ components.

The solution of a MOO problem –Pareto Set and Pareto Front– is based on the concept of dominance.

Definition 2.1. Dominance (Pareto (1971)): A decision vector $\boldsymbol{x^1}$ is dominated by a decision vector $\boldsymbol{x^2}$ if $f_i(\boldsymbol{x^2}) \leq f_i(\boldsymbol{x^1})$ for all $i \in [1, ..., m]$ and $f_j(\boldsymbol{x^2}) < f_j(\boldsymbol{x^1})$ for at least one j, $j \in [1, ..., m]$. This is denoted as $\boldsymbol{x^2} \preceq \boldsymbol{x^1}$.

Definition 2.2. Pareto set P_Q: is the set of solutions in Q that is non dominated by any solution in Q.

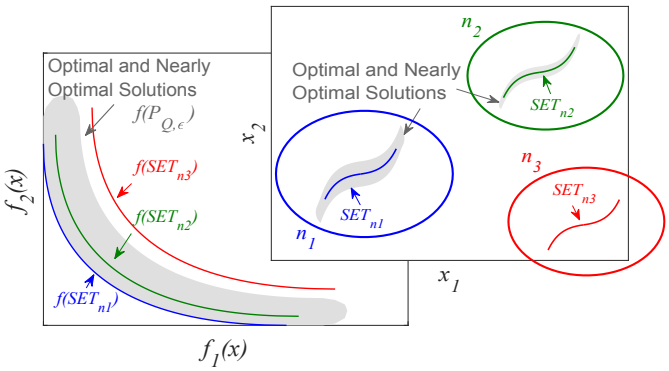

Fig. 1. The optimal solutions are the ones in set SET_{n1} (blue front) and the nearly optimal solutions non dominated in their neighborhood are the ones in SET_{n2} (green front).

Definition 2.3. Pareto front $\boldsymbol{f}(P_Q)$: set of values in objective space corresponding to the Pareto set P_Q.

For the handling of nearly optimal solutions some additional definitions are necessary:

Definition 2.4. $-\epsilon$-dominance (Schütze et al. (2007)): Define $\boldsymbol{\epsilon} = [\epsilon_1, ..., \epsilon_m]$ as the maximum acceptable performance degradation. A decision vector $\boldsymbol{x^1}$ is $-\epsilon$-dominated by another decision vector $\boldsymbol{x^2}$ if $f_i(\boldsymbol{x^2}) + \epsilon_i \leq f_i(\boldsymbol{x^1})$ for all $i \in [1, ..., m]$ and $f_j(\boldsymbol{x^2}) + \epsilon_i < f_j(\boldsymbol{x^1})$ for at least one j, $j \in [1, ..., m]$. This is denoted by $\boldsymbol{x^2} \preceq_{-\epsilon} \boldsymbol{x^1}$.

Definition 2.5. ϵ-efficiency (Schütze et al. (2011)): The set of ϵ-efficient solutions ($P_{Q,\epsilon}$) is the set of solutions in Q which are not $-\epsilon$-dominated by any solution in Q.

And finally, the concept of neighborhood and how it modifies the concept of dominance has to be defined.

Definition 2.6. Neighborhood: Define $\boldsymbol{n} = [n_1, ..., n_k]$ as the maximum distance between neighboring solutions. Two decision vectors $\boldsymbol{x^1}$ and $\boldsymbol{x^2}$ are neighboring solutions ($\boldsymbol{x^1} =_n \boldsymbol{x^2}$) if $|x_i^1 - x_i^2| < n_i$ for all $i \in [1, ..., k]$.

Definition 2.7. ($n-$dominance): A decision vector $\boldsymbol{x^1}$ is $n-$dominated by a decision vector $\boldsymbol{x^2}$ if they are neighboring solutions (Definition 2.6) and $\boldsymbol{x^2} \preceq \boldsymbol{x^1}$. This is denoted by $\boldsymbol{x^2} \preceq_n \boldsymbol{x^1}$.

Definition 2.8. ($n-$efficiency): The set of $n-$efficient solutions ($P_{Q,n}$) is the set of solutions of $P_{Q,\epsilon}$ which are not $n-$dominated by another solution in $P_{Q,\epsilon}$.

Figure 1 shows an example to illustrate (in bi-objective case) the optimal, nearly optimal, and nearly optimal solutions non dominated in their neighborhood. The figure shows a set of optimal and nearly optimal solutions $P_{Q,\epsilon}$ (gray areas). There is a set of optimal solutions SET_{n1} that are in the neighborhood n_1 and a set of nearly optimal solutions SET_{n2} in a different neighborhood n_2. The neighborhood n_3 is discarded because it does not contain any nearly optimal solution. Then in this case $P_{Q,n}$ is $SET_{n1} \cup SET_{n2}$. Generally, the algorithms try to obtain a discrete set $P^*_{Q,n} \subset P_{Q,n}$, in such a way that $P^*_{Q,n}$ appropriately characterizes $P_{Q,n}$. This is because determining $P_{Q,n}$ is usually unapproachable, since it may have infinite solutions (note that the set $P^*_{Q,n}$ is not unique).

3. *nevMOGA* ALGORITHM

In this work the evolutionary algorithm nevMOGA (Pajares et al. (2018)) is applied to characterize the discrete set of optimal and nearly optimal solutions non dominated in their neighborhood. This set is defined as the set of $n-$efficient options ($P_{Q,n}$, see Definition 2.8).

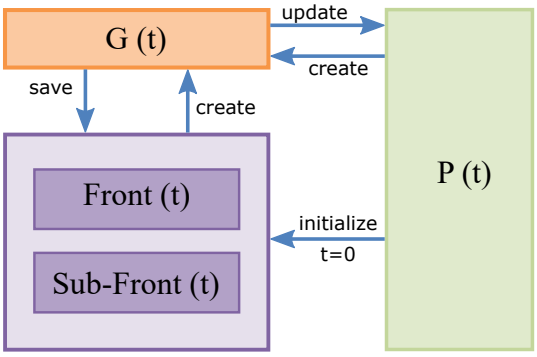

Fig. 2. Structure of nevMOGA formed by four populations.

nevMOGA manages four populations (see Figure 2):

(1) P(t) is the main population. This population converges towards $P_{Q,n}$ and not only on P_Q.
(2) Front(t) is the archive where P_Q^* is stored, i.e., a discrete approximation of the Pareto front.
(3) Sub-front(t) is the archive where $P_{Q,n}^* \setminus P_Q^*$ is stored, i.e., a discrete approximation of the nearly optimal solutions non dominated in their neighborhood.
(4) G(t) is an auxiliary population where the new individuals generated by evolutionary techniques in each iteration are stored.

Algorithm 1 shows the pseudocode for nevMOGA. It is an algorithm based on evolutionary methods in which the following operations can be highlighted:

- Line 6 and 15, ranks P(t) according to the population density in each individual's environment.
- Line 10, the population G(t) is created by evolutionary operators (selection, crossover and mutation).
- Incorporating solutions in the different subpopulations (lines 7, 8, 12, 13 and 14) is carried out using functions based on definitions described in section 2.

The details of the algorithm and the setting of its parameters can be found in (Pajares et al. (2018)).

4. IDENTIFICATION OF THE COOLING SUBSYSTEM OF A μ-CHP SYSTEM BASED ON A PEMFC

The model to be identified described in (Navarro Giménez et al. (2019)) is based on first principles and has a non linear structure. The model will be adjusted and validated with experimental data obtained from a real process that simulates a μ-CHP system based on PEMFC. Details of this model as well as the data sets used for its identification and validation can be seen in (Navarro Giménez et al. (2019)). The inputs model are (in red in Figure 3):

- F_a: PEMFC air flow, m^3/s
- T_{amb}: Ambient temperature, ^oC

Algorithm 1 Main pseudocode.

```
1: t:=0;
2: Front(t):= ∅;
3: Sub-Front(t):= ∅;
4: Create initial population P(t) at random
5: Calculate f(x) ∀ x ∈ P(t)
6: Rank population P(t)
7: Inclusion of the individuals of P(t) in Front(t)
8: Inclusion of the individuals of P(t) ∉ Front(t) in Sub-Front(t)
9: for t:= 1:Number of iterations do
10:    Create population G(t)
11:    Calculate f(x) ∀ x ∈ G(t)
12:    Inclusion of the individuals of G(t) in Front(t)
13:    Inclusion of the individuals of G(t) ∉ Front(t) in Sub-Front(t)
14:    Update P(t) with the individuals of G(t)
15:    Rank population P(t)
16: end for
```

- $T_{a_{in}}$: PEMFC air inlet temperature, ^oC
- v: Voltage supplied by the PEMFC, V.
- i: Current supplied by the PEMFC, A.
- F_{w_1}: Primary circuit flow rate, m^3/s.
- F_{w_2}: Secondary circuit flow rate, m^3/s.
- R: Radiator, on/off.

The outputs of the model are (in blue in the Figure 3):

- $T_{w_{out}}$: PEMFC water outlet temperature, ^oC.
- $T_{w_{in}}$: PEMFC water inlet temperature, ^oC.
- T_{t2}: Temperature inside the tank 2, ^oC,
- $T_{a_{out}}$: PEMFC outlet air temperature, ^oC.
- $T_{s_{in}}$: Shell exchanger inlet water temperature, ^oC.
- $T_{s_{out}}$: Shell exchanger outlet water temperature, ^oC.

Fig. 3. Inputs and outputs of the a μ-CHP cooling system.

The model has 30 parameters to estimate. To adjust them, the identification data set (approximately 2.5h long) performed on the real plant will be used (see Figure 4 in Navarro Giménez et al. (2019)). In this test, steps are introduced in the electricity demand, the flows of primary and secondary circuits of the cooling system, and the demand for thermal energy. Additionally, there is a validation data set (Figure 5 in Navarro Giménez et al. (2019)).

4.1 MOO problem

The MOO problem is defined as follows:

$$\min_{\boldsymbol{x}} \boldsymbol{f}(\boldsymbol{x}) = [f_1(\boldsymbol{x})\ f_2(\boldsymbol{x})\ f_3(\boldsymbol{x})] \tag{3}$$

subject to $\underline{\boldsymbol{x}} \leq \boldsymbol{x} \leq \overline{\boldsymbol{x}}$ where:

$$f_1 = \frac{1}{T}\int_0^T \left|\hat{T}_{w_{out}}(t) - T_{w_{out}}(t)\right| dt \tag{4}$$

$$f_2 = \frac{1}{T}\int_0^T \left|\hat{T}_{w_{in}}(t) - T_{w_{in}}(t)\right| dt \tag{5}$$

Table 1. Lower ($\underline{\boldsymbol{x}}$) and upper ($\overline{\boldsymbol{x}}$) limits of the cooling system parameters.

Parameter	$\underline{\boldsymbol{x}}$	$\overline{\boldsymbol{x}}$	Parameter	$\underline{\boldsymbol{x}}$	$\overline{\boldsymbol{x}}$
V_{t1}	0.001	0.003	$h_{w_{max}}$	1	200
$h_{t_{min}}$	1	100	$h_{w_{min}}$	1	150
$h_{t_{max}}$	1	200	h_{aw}	1	100
$h_{s_{min}}$	1	150	$cal_{T_{w_{out}}}$	-2	2
$h_{s_{max}}$	1	300	$cal_{T_{a_{out}}}$	-2	2
V_{p1}	0.0001	0.001	V_{p4}	0.001	0.002
$h_{p1_{loss}}$	1	15	$h_{p4_{loss}}$	1	14
V_w	0.001	0.004	$cal_{T_{p4_{out}}}$	-2	2
V_a	0.001	0.005	$h_{r_{OFFmin}}$	1	40
k_a	1000	8000	$h_{r_{OFFmax}}$	1	40
$h_{fc_{2max}}$	1	100	$h_{r_{ONmin}}$	1	100
$h_{fc_{2min}}$	1	100	$h_{r_{ONmax}}$	1	200
$h_{fc_{loss}}$	1	15	V_{t2}	0.015	0.035
$h_{a_{max}}$	1	150	V_r	0.001	0.005
$h_{a_{min}}$	1	100	T_{amb_r}	15	35

$$f_3 = \frac{1}{T}\int_0^T \left|\hat{T}_{t2}(t) - T_{t2}(t)\right| dt \tag{6}$$

$T = 8087s$ is the duration of the identification test, variables with and without circumflex accent are process and model outputs respectively, $\boldsymbol{x}$ is the parameter vector

$$\boldsymbol{x} = [V_{t1}\ h_{t_{min}}\ h_{t_{max}}\ h_{s_{min}}\ h_{s_{max}}\ V_{p1}\ h_{p1_{loss}}\ V_w\ V_a\ k_a\ h_{fc_{2max}}\ h_{fc_{2min}}\ h_{fc_{loss}}\ h_{a_{max}} h_{a_{min}}\ h_{w_{max}}\ h_{w_{min}}\ h_{aw}\ cal_{T_{w_{out}}}\ cal_{T_{a_{out}}}\ V_{p4}\ h_{p4_{loss}}\ cal_{T_{p4_{out}}}\ h_{r_{OFFmin}}\ h_{r_{OFFmax}}\ h_{r_{ONmin}}\ h_{r_{ONmax}}\ V_{t2}\ V_r\ T_{amb_r}] \tag{7}$$

and $\underline{\boldsymbol{x}}$ and $\overline{\boldsymbol{x}}$ (see Table 1) the lower and upper limits of $\boldsymbol{x}$. The design objectives measure the error, along the aforementioned identification test, at water temperatures: inlet and outlet water ($T_{w_{in}}$ and $T_{w_{out}}$ respectively) and reservoir 2 (T_{t2}). The PEMFC outlet air temperatures ($T_{a_{out}}$), and inlet and outlet temperatures in the heat exchanger shell ($T_{s_{in}}$ and $T_{s_{out}}$ respectively) are less important model outputs. Therefore, the error associated with these signals has not been included in the design objectives. In this way, the MOO problem is reduced to 3 objectives in order to reduce the optimization process and the analysis of the models obtained. So, we facilitate the convergence of nevMOGA, not considering the objectives that are less important for the designer. However, the errors in these outputs (objectives f_4, f_5 and f_6, see Equation 8) will be analyzed in the decision phase.

$$\begin{aligned} f_4 &= \frac{1}{T}\int_0^T \left|\hat{T}_{a_{out}}(t) - T_{a_{out}}(t)\right| dt \\ f_5 &= \frac{1}{T}\int_0^T \left|\hat{T}_{s_{out}}(t) - T_{s_{out}}(t)\right| dt \\ f_6 &= \frac{1}{T}\int_0^T \left|\hat{T}_{s_{in}}(t) - T_{s_{in}}(t)\right| dt \end{aligned} \tag{8}$$

To optimize the defined MOO problem, nevMOGA with the following configuration is used:

- $Nind_G = 4$ (size population G)
- $Nind_P = 250$ (size population P)
- $Iterations = 1000$
- $\boldsymbol{\epsilon} = [0.01\ 0.01\ 0.01]$ (objective degradation accepted)
- $\boldsymbol{n} = [0.0005\ 10\ 20\ 10\ 40\ 0.0003\ 4\ 0.0005\ 0.0001\ 1000\ 15\ 15\ 3\ 15\ 10\ 15\ 15\ 15\ 0.5\ 0.5\ 0.0005\ 4\ 0.2\ 5\ 7\ 7\ 10\ 0.002\ 0.0004\ 3]$ (neighborhood definition)

In this MOO problem the decision variables and objectives have a physical sense which facilitates the choice of the parameters of nevMOGA ($\boldsymbol{\epsilon}$ and $\boldsymbol{n}$), the analysis and the decision making process. Figure 4 shows the set of models obtained ($P_{Q,n}$) using nevMOGA for the proposed MOO problem. Given the large number of dimensions in objective and decision spaces, the Level Diagrams (LD) tool (Blasco et al. (2017)) has been used for graphical representation.

The LD tool transforms the m-dimensional objective space and the k-dimensional decision space into $m + k$ two-dimensional separate but synchronized graphs. LD provides a two-dimensional graph for each objective and decision variable. On the abscissa axis of each graph, the values for each objective or decision variable are represented, while the ordinate axes of all graphs display the p-norm calculated for each solution. In particular, for Figure 4, 2-norm is used ($||\cdot||_2$). This allows graphics to stay synchronized by means of their ordinate axes —meaning that each given solution presents identical ordinate value in every graph— and, therefore, helps to compare solutions according to the selected norm. For more details about this representation see (Blasco et al. (2008)) or (Blasco et al. (2017)).

Starting the LD analysis, the Pareto front (orange color solutions) in Figure 4 shows a trade-off between objectives (expected due to the non-modeled dynamics). It is possible to achieve prediction errors near to 0.1^oC in f_1 but increasing f_3 to values of 0.3^oC. Besides, there are a large number of nearly optimal models (green color solutions) with similar performance to the optimal ones. To compare their performance, two of them are chosen. Firstly, model $\boldsymbol{x^1}$ is selected from the Pareto front. $\boldsymbol{x^1}$ gets the lowest value of norm 2 (ordinate axis of Figure 4). This alternative is a balanced model, and could be the final choice of the designer. Secondly, a nearly optimal solution ($\boldsymbol{x^2}$) dominated by $\boldsymbol{x^1}$ is selected, but in a different neighborhood, that is, significantly different (see Table 2).

The response of the models $\boldsymbol{x^1}$ and $\boldsymbol{x^2}$ on the identification test is shown in Figure 5. Besides, the objective values for both models are shown in the Table 3. The model $\boldsymbol{x^1}$ has an error slightly lower than $\boldsymbol{x^2}$, in all objectives (f_1 to f_3).

Analyzing in deep the time response (see Figure 5) it can been noticed zones where model x^1 adjusts better the behavior of the process than x^2 one (see instant of time around $3000s$). However there are other areas where the opposite occurs (see time instant around $4200s$). This shows that different models can produce similar values of the design objectives even presenting clear differences in different zones of the experiment. Therefore, the identification problem is a multimodal optimization problem.

On the other hand, since these two models have very similar performance, it seems appropriate to analyze new objectives in order to be able to make a better informed decision. First, in Figure 6 the evolution of the less significant outputs ($T_{a_{out}}$, $T_{s_{in}}$ and $T_{s_{out}}$) for both models on the identification test is shown. It is observed how the nearly optimal model $\boldsymbol{x^2}$ improves the performance (lower error) with respect to the optimal model $\boldsymbol{x^1}$ (see also the value of the objectives f_4, f_5 and f_6 in the Table 3). This

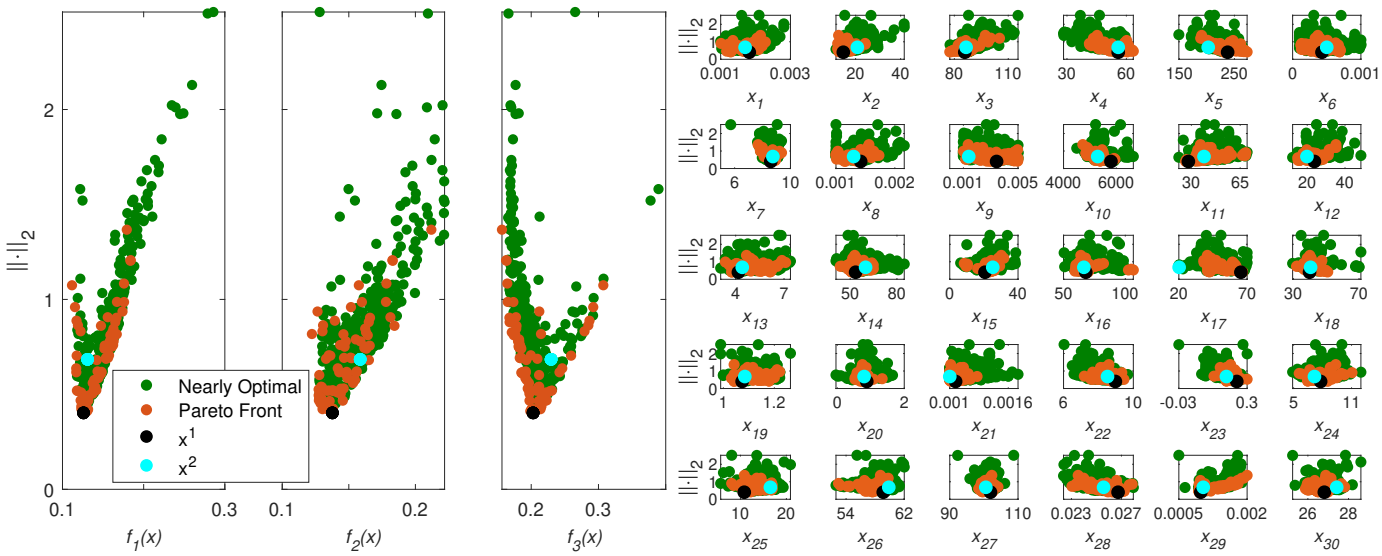

Fig. 4. Approximation to the set of optimal models (orange) and nearly optimal models non dominated in their neighborhood (green). The models are represented by means of the LD visualization tool, using 2-norm ($||\cdot||_2$). On the left, the objective value of the solutions are shown. On the right, the model parameters x_1 to x_{30} are shown.

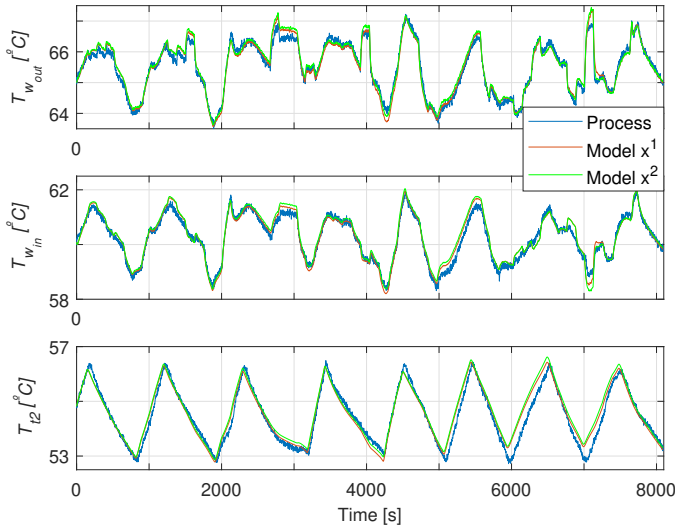

Fig. 5. Outputs $T_{w_{out}}$, $T_{w_{in}}$ and T_{t2} obtained for the models $\boldsymbol{x^1}$ and $\boldsymbol{x^2}$ on the identification test. The error of these outputs on the identification test is evaluated in the design objectives f_1, f_2 and f_3. (see Table 3).

improvement is significant with respect to the output $T_{a_{out}}$ (objective f_4).

Secondly, we observe in Figure 7 the response of the six model outputs on the validation test. The nearly optimal model $\boldsymbol{x^2}$ improves the performance, in all outputs, compared to model $\boldsymbol{x^1}$ (see the objective values in the Table 4) on the validation data set. This improvement is significant, again, in the output $T_{a_{out}}$ (f_4). So, $\boldsymbol{x^1}$ and $\boldsymbol{x^2}$ are two significantly different models with very similar performance in the design objectives. $\boldsymbol{x^1}$ model gets a slightly higher performance. However, with respect to other objectives (errors concerning the outputs $T_{a_{out}}$, $T_{s_{in}}$ and $T_{s_{out}}$), the model $\boldsymbol{x^2}$ obtains better performance than $\boldsymbol{x^1}$, there is a significant improvement with respect to the output $T_{a_{out}}$. In addition, with respect to the validation test, the model $\boldsymbol{x^2}$ improves the optimal model $\boldsymbol{x^1}$ in all the outputs, and

Table 2. Models $\boldsymbol{x^1}$ and $\boldsymbol{x^2}$.

Parameter	$\boldsymbol{x^1}$	$\boldsymbol{x^2}$	Parameter	$\boldsymbol{x^1}$	$\boldsymbol{x^2}$
V_{t1}	0.0018	0.0017	$h_{w_{max}}$	68	66.45
$h_{t_{min}}$	14.55	20.78	$h_{w_{min}}$	65.45	20.21
$h_{t_{max}}$	85.8	86.54	h_{aw}	39.9	40.53
$h_{s_{min}}$	55.89	55.88	$cal_{T_{w_{out}}}$	1.08	1.09
$h_{s_{max}}$	237.67	202.39	$cal_{T_{a_{out}}}$	0.88	0.8
V_{p1}	0.00043	0.0005	V_{p4}	0.0011	0.001
$h_{p1_{loss}}$	8.59	8.74	$h_{p4_{loss}}$	8.97	8.52
V_w	0.0014	0.0013	$cal_{T_{p4_{out}}}$	0.25	0.2
V_a	0.0034	0.0014	$h_{r_{OFFmin}}$	7.8	7.16
k_a	5799.3	5295.8	$h_{r_{OFFmax}}$	10.83	16.52
$h_{fc_{2max}}$	27.83	39.05	$h_{r_{ONmin}}$	59.12	59.88
$h_{fc_{2min}}$	23.8	19.86	$h_{r_{ONmax}}$	101.93	100.57
$h_{fc_{loss}}$	4.17	4.41	V_{t2}	0.0267	0.0256
$h_{a_{max}}$	53.49	59.89	V_r	0.001	0.0011
$h_{a_{min}}$	20.64	25.19	T_{amb_r}	26.81	27.42

Table 3. Value of the defined objectives for the models $\boldsymbol{x^1}$ and $\boldsymbol{x^2}$ for the identification test.

Model	f_1	f_2	f_3	f_4	f_5	f_6
$\boldsymbol{x^1}$	**0.126**	**0.138**	**0.203**	0.805	0.200	0.178
$\boldsymbol{x^2}$	0.131	0.159	0.230	**0.405**	**0.167**	**0.170**

Table 4. Value of the objectives for the models $\boldsymbol{x^1}$ and $\boldsymbol{x^2}$ for the validation test.

Model	f_1	f_2	f_3	f_4	f_5	f_6
$\boldsymbol{x^1}$	0.742	0.639	0.447	1.231	0.816	0.642
$\boldsymbol{x^2}$	**0.726**	**0.629**	**0.406**	**0.827**	**0.786**	**0.603**

in particular for output $T_{a_{out}}$. Therefore, the model $\boldsymbol{x^2}$ is selected as the final solution of the MOO problem.

5. CONCLUSIONS

The work presented shows the benefits of finding the optimal and near optimal solutions in an identification problem set as a MOO. In addition, identification problems

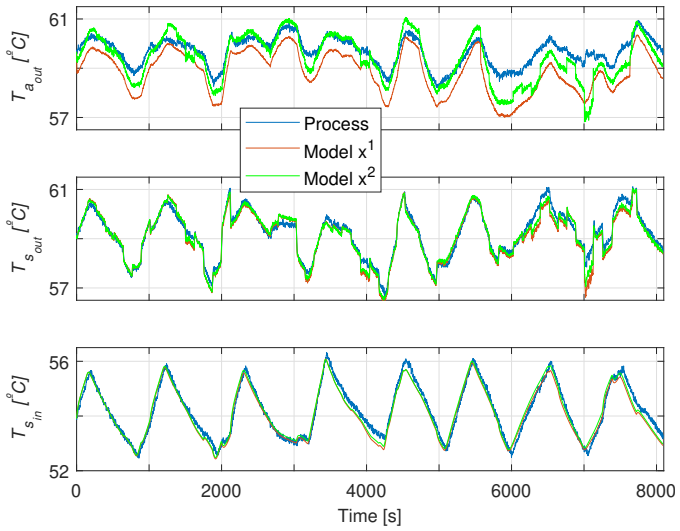

Fig. 6. Outputs $T_{a_{out}}$, $T_{s_{in}}$ and $T_{s_{out}}$ obtained for the models $\boldsymbol{x^1}$ and $\boldsymbol{x^2}$ on the identification data set. The error of these outputs on the identification data set is evaluated in the objectives f_4, f_5 and f_6 (see Table 3).

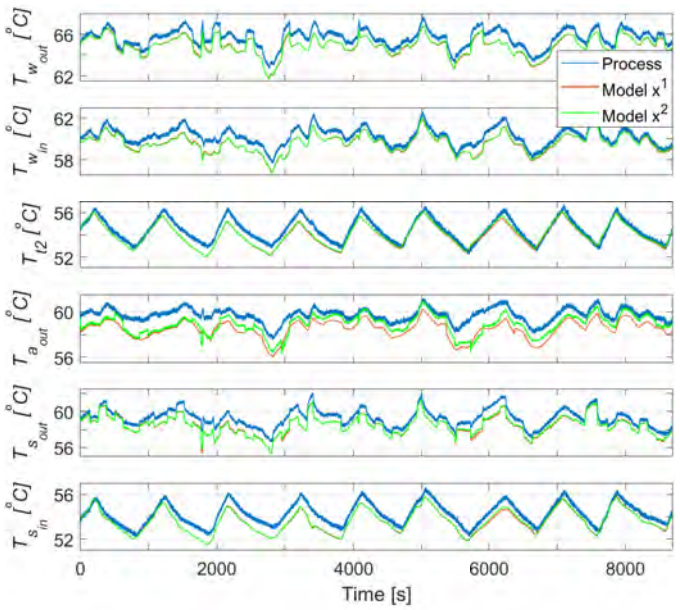

Fig. 7. Outputs $T_{w_{out}}$, $T_{w_{in}}$, T_{t2}, $T_{a_{out}}$, $T_{s_{in}}$ and $T_{s_{out}}$ obtained for the models $\boldsymbol{x^1}$ and $\boldsymbol{x^2}$ on the validation test. The error of these outputs on the validation test is evaluated in the objectives f_1 to f_6 (see Table 4).

have been shown to be multimodal optimization problems, and significantly different optimal solutions may exist.

By obtaining the set of near-optimal solutions not dominated in their neighborhood, the designer

1) Obtains models with performances similar to the optimal models but with significantly different characteristics.

2) Can carry out a detailed analysis considering extra objectives and validation experiments.

In this paper, we have analyzed two significantly different solutions in the parameter space. In this study we have seen how their different responses provide diversity to the designer, despite the predominance of one over the other with respect to the design objectives. However, the analysis of the parametric space, in this case, is complex due to the large number of decision variables. Using this approach, the designer can take the final decision with information that would not have been obtained with the traditional multiobjective optimization approach.

As future work, it is possible to perform a deeper analysis of the set of models obtained through nevMOGA (including the analysis in the parameter space). In addition, it is possible to apply this approach to other engineering problems. In the same way, it is also possible to improve the nevMOGA algorithm. Such improvements can be aimed, for example, to reduce its computation cost or to use clustering techniques for the choice of the neighborhood (sometimes difficult for the designer).

REFERENCES

Blasco, X., Herrero, J., Sanchis, J., and Martínez, M. (2008). A new graphical visualization of n-dimensional pareto front for decision-making in multiobjective optimization. *Information Sciences*, 178(20), 3908– –3924.

Blasco, X., Herrero, J.M., Reynoso-Meza, G., and Iranzo, M.A.M. (2017). Interactive tool for analyzing multiobjective optimization results with level diagrams. In *Proceedings of the Genetic and Evolutionary Computation Conference Companion*, 1689–1696. ACM.

Coello, C.A.C., Lamont, G.B., Van Veldhuizen, D.A., et al. (2007). *Evolutionary algorithms for solving multi-objective problems*, volume 5. Springer.

Hawkes, A., Staffell, I., Brett, D., and Brandon, N. (2009). Fuel cells for micro-combined heat and power generation. *Energy & Environmental Science*, 2(7), 729–744.

Maghanki, M.M., Ghobadian, B., Najafi, G., and Galogah, R.J. (2013). Micro combined heat and power (MCHP) technologies and applications. *Renewable and Sustainable Energy Reviews*, 28, 510–524.

Miettinen, K. (1998). *Nonlinear Multiobjective Optimization*. Kluwer Academic Publishers.

Navarro Giménez, S., Herrero Durá, J.M., Blasco Ferragud, F.X., and Simarro Fernández, R. (2019). Control-oriented modeling of the cooling process of a PEMFC-based μ-CHP system. *IEEE Access*, 7, 95620–95642.

Pajares, A., Blasco, X., Herrero, J.M., and Reynoso-Meza, G. (2018). A multiobjective genetic algorithm for the localization of optimal and nearly optimal solutions which are potentially useful: nevMOGA. *Complexity*, 2018.

Pareto, V. (1971). *Manual of political economy*. AM Kelley.

Schmittinger, W. and Vahidi, A. (2008). A review of the main parameters influencing long-term performance and durability of pem fuel cells. *Journal of power sources*, 180(1), 1–14.

Schütze, O., Coello, C.A.C., and Talbi, E.G. (2007). Approximating the ε-efficient set of an mop with stochastic search algorithms. In *Mexican International Conference on Artificial Intelligence*, 128–138. Springer.

Schütze, O., Vasile, M., and Coello, C.A.C. (2011). Computing the set of epsilon-efficient solutions in multiobjective space mission design. *Computing*, 8.